Inorg. Chem. **2002**, *41*, 513–520

Trithiotungsten(VI) Complexes Having Phosphine-Thiolate Hybrid Ligands: Synthesis and Cluster Forming Reactions with CuBr, $FeCl_2$, and $[Fe(CH_3CN)_6](ClO_4)_2$

Yasuhiro Arikawa,[†] Hiroyuki Kawaguchi,[‡] Kazuo Kashiwabara,[†] and Kazuyuki Tatsumi*,[†]

Research Center for Materials Science and Department of Chemistry, Graduate School of Science, Nagoya University, Furo-cho, Chikusa-ku, Nagoya 464-8602, Japan, and Coordination Chemistry Laboratories, Institute for Molecular Science, Myodaiji, Okazaki 444-8595, Japan

Received August 24, 2001

Five-coordinated trithiotungsten complexes $(PPh_4)[(dmsp)W(S)_3]$ (**1a**) and $(PPh_4)[(dpsp)W(S)_3]$ (**1b**) ($R_2PCH_2CH_2S^-$; R = Me (dmsp$^-$), Ph (dpsp$^-$)) were synthesized by addition of Hdmsp and Hdpsp to a THF solution of $(PPh_4)[(EtS)W(S)_3]$. Treatment of **1a** with CuBr in the presence of PPh_3 in CH_3CN afforded a WCu_2 cluster $(dmsp)WS_3Cu_2(PPh_3)_2Br$ (**2**). The reaction of **1a** with 1 equiv of $FeCl_2$ went smoothly to generate a 1:1 adduct $(PPh_4)[(dmsp)WS_3(FeCl_2)]$ (**3**), while **3** did not react further with excess $FeCl_2$. On the other hand, **3** was found to react with $[Fe(CH_3CN)_6](ClO_4)_2$, giving rise to an unusual tetranuclear cluster, $[(dmsp)WS_3]_2Fe_2Cl$ (**4**), while the reaction of **1a** with 2 equiv of $[Fe(CH_3CN)_6](ClO_4)_2$ led to a cyclic octanuclear cluster $[(dmsp)WS_3Fe]_4$ (**5**). Although the oxidation states of W(VI), Cu(I), and Fe(II) are retained in **2** and **3**, reduction of the metal ions occurs in the formation of **4** and **5**. All the complexes reported in this paper were structurally characterized by X-ray analysis. It is anticipated that the new type of trithiotungsten complexes, **1a** and **1b**, will serve as potential synthons for various heterometallic sulfide clusters.

Introduction

Tetrathiometalates formulated as $[M(S)_4]^{n-}$ (M = V, Nb, Ta, n = 3;[1] M = Mo, W, n = 2;[2] M = Re, n = 1[3]) have been recognized as key entities in developing the chemistry of transition metal sulfide clusters. The presence of M═S multiple bonds is important in cluster forming reactions, because the terminal sulfides readily capture other metal atoms owing to the ability of a sulfur atom to bridge two or three metal centers. Aside from tetrathiometalates and analogous trithiometalates, however, transition metal complexes carrying two[4] or more terminal sulfides are still rare. Recently, the reactions of $(Et_4N)[(R_2Tp)W(CO)_3]$ (R = H, HB(pyrazol-1-yl)$_3$; R = CH_3, HB(3,5-dimethylpyrazol-1-yl)$_3$)

* To whom correspondence should be addressed. E-mail: i45100a@nucc.cc.nagoya-u.ac.jp. Fax: +81-52-789-2943.

† Nagoya University.

‡ Institute for Molecular Science.

(1) (a) Do, Y.; Simhon, E. D.; Holm, R. H. *J. Am. Chem. Soc.* **1983**, *105*, 6731−6732. (b) Do, Y.; Simhon, E. D.; Holm, R. H. *Inorg. Chem.* **1985**, *24*, 4635−4642. (c) Lee, S. C.; Holm, R. H. *J. Am. Chem. Soc.* **1990**, *112*, 9654 − 9655. (d) Lee, S. C.; Li, J.; Mitchell, J. C.; Holm, R. H. *Inorg. Chem.* **1992**, *31*, 4333−4338. (e) Müller, A.; Schimanski, J.; Bögge, H. *Z. Anorg. Allg. Chem.* **1987**, 544, 107−114. (f) Scattergood, C. D.; Bonney, P. G.; Slater, J. M.; Garner, C. D.; Clegg, W. *Chem. Commun.* **1987**, 1749−1750. (g) Yang, Y.; Liu, Q.; Huang, L.; Wu, D.; Kang, B.; Lu, J. *Inorg. Chem.* **1993**, *32*, 5431−5432. (h) Cen, W.; Lee, S. C.; Li, J.; MacDonnell, F. M.; Holm, R. H. *J. Am. Chem. Soc.* **1993**, *115*, 9515−9523. (i) Liu, Q.; Yang, Y.; Huang, L.; Wu, D.; Kang, B.; Chen, C.; Deng, Y.; Lu, J. *Inorg. Chem.* **1995**, *34*, 1884−1893. (j) Yu, X.-F.; Zheng, F.-K.; Huang, L.-R. *Polyhedron* **1995**, *14*, 3599−3604. (k) Canales, F.; Gimeno, M. C.; Leguna, A. *Inorg. Chem.* **1998**, *37*, 5376−5379.

(2) (a) Müller, A.; Diemann, E.; Jostes, R.; Bögge, H. *Angew. Chem., Int. Ed. Engl.* **1981**, *20*, 934−955. (b) Christou, G.; Garner, C. D.; Mabbs, F. E.; King, T. J. *J. Chem. Soc., Chem. Commun.* **1978**, 740−741. (c) Coucouvanis, D. *Acc. Chem. Res.* **1981**, *14*, 201−209. (d) Howard, K. E.; Rauchfuss, T. B.; Wilson, J. R. *Inorg. Chem.* **1988**, *27*, 3561−3567. (e) Jeannin, Y.; Sécheresse, F.; Bernes, S.; Robert, F. *Inorg. Chim. Acta* **1992**, *198*−*200*, 493−505. (f) Evans, W. J.; Ansari, M. A.; Ziller, J. W.; Khan, S. I. *Organometallics* **1995**, *14*, 3−4. (g) Hou, H.-W.; Xin, X.-Q.; Shi, S. *Coord. Chem. Rev.* **1996**, *153*, 25−56. (h) Lang, J.; Tatsumi, K.; *Inorg. Chem.* **1998**, *37*, 6308−6316. (i) Ogo, S.; Suzuki, T.; Ozawa, Y.; Isobe, K. *Inorg. Chem.* **1996**, *35*, 6093−6101.

(3) (a) Müller, A.; Krickemeyer, E.; Bögge, H. *Angew. Chem., Int. Ed. Engl.* **1986**, *25*, 990−991. (b) Müller, A.; Krickemeyer, E.; Bögge, H. *Z. Anorg. Allg. Chem.* **1987**, *554*, 61−78. (c) Clegg, W.; Garner, C. D.; Scattergood, C. D. *Acta Crystallogr., Sect. C* **1988**, *44*, 753−755. (d) Ciurli, S.; Carney, M. J.; Holm, R. H.; Papaefthymiou, G. C. *Inorg. Chem.* **1989**, *28*, 2696−2698. (e) Müller, A.; Krickemeyer, E.; Penk, M. *J. Chem. Soc., Chem. Commun.* **1990**, 321−322. (f) Ciurli, S.; Holm, R. H. *Inorg. Chem.* **1991**, *30*, 743−750. (g) Müller, A.; Krickemeyer, E.; Hildebrand, A.; Bögge, H.; Schneider, K.; Lemke, M. *J. Chem. Soc., Chem. Commun.* **1991**, 1685−1687. (h) Müller, A.; Hildebrand, A.; Krickemeyer, E.; Khan, M. I.; Penk, M.; Bögge, H.; Sécheresse, F. *Chem.—Eur. J.* **1998**, *4*, 1932−1937.

10.1021/ic010921q CCC: $22.00
Published on Web 12/29/2001

with elemental sulfur were reported to generate trithiotungsten complexes, $(Et_4N)[(R_2Tp)W(S)_3]$.[5] In our laboratory, a series of half-sandwich trithio complexes, $[Cp^*M(S)_3]^{n-}$ ($Cp^* = C_5Me_5$, M = Ta, Nb, $n = 2$;[6a,b] M = Mo, W, $n = 1$[6c,d]), have been synthesized, and they proved to be useful precursors for a large variety of heterometallic sulfide clusters.[7]

Another interesting family of this class are monoalkylated tetrathiotungstates $(PPh_4)[(RS)W(S)_3]$ (R = Et, ^{i}Pr, ^{i}Bu, ^{t}Bu, benzyl, allyl, *n*-hexyl), which have been isolated first by Boorman et al. and later by us.[8,9] The analogous trithio(thiolato) complexes of niobium and tantalum, $(Et_4N)_2[(^tBuS)M(S)_3]$ (M = Nb, Ta), were prepared from the reactions of $NbCl_5$ and $TaCl_5$ with NaS^tBu in the presence of elemental sulfur.[10] A unique aspect of these complexes is that they are electronically/coordinatively unsaturated, as one multiple M═S bond of tetrathiometalates is replaced by a single M−SR bond. Because of the electronic/coordinative unsaturation, the tungsten complexes in particular tend to degradate in solution via complicated ligand exchange and/or redox processes. Probably because of the propensity for degradation, utility of $(PPh_4)[(RS)W(S)_3]$ for cluster synthesis has yet to be realized. As a matter of fact, when we treated $(PPh_4)[(EtS)W(S)_3]$ with $FeCl_2$ in CH_3CN, disproportionation reaction seemed to occur, and $(PPh_4)_2[WS_4(FeCl_2)_2]$ was the sole isolable product.[11]

We sensed that monoalkylated tetrathiotungstates would be stabilized by a thiolate ligand having an additional O-donor site which might coordinate to the electron-deficient W(VI) center. Thus, the reactions of $(PPh_4)_2[W(S)_4]$ with 2-(bromomethyl)tetrahydro-2H-pyran (Br-mthp) and 2-(bromoethyl)-1,3-dioxane (Br-edo) were carried out, and the alkylated complexes, $(PPh_4)[(mthp\text{-}S)W(S)_3]$ and $(PPh_4)[(edo\text{-}S)W(S)_3]$, were isolated.[9] Contrary to our expectation, however, the X-ray structures showed that the O-donors of mthp-S and edo-S did not coordinate at W(VI).

Now, our efforts focus on attempts to prepare trithiotungsten complexes having phosphine-thiolato hybrid ligands, $R_2PCH_2CH_2S^-$ (R = Me (dmsp$^-$), Ph (dpsp$^-$)),[12] expecting that phosphine in the proximity of a thiolate sulfur may be bound to W(VI) more strongly than O-donors. Previously, we synthesized a dmsp complex of molybdenum, $Mo(dmsp)_2(S^tBu)_2$, by ligand exchange reaction of $Mo(S^tBu)_4$ with Hdmsp. This complex was found to react with $FeCl_2$ and CuBr to give $[Mo(O)(dmsp)_2]_2FeCl_2$ and $[MoBr(dmsp)_2(\mu_3\text{-}S)Cu_2]_2(\mu_2\text{-}S^tBu)_2$, respectively.[13] This paper reports the successful synthesis of trithiotungsten complexes bearing dmsp and dpsp ligands and shows that coordination of phosphine in fact increases stability of the trithio(thiolato) structures in solution, allowing us to examine cluster forming reactions with CuBr, $FeCl_2$, and $[Fe(CH_3CN)_6](ClO_4)_2$.

Experimental Section

General. All manipulations were carried out under argon using standard Schlenk-line techniques. Solvents were predried over activated molecular sieves and refluxed over the appropriate drying agents under dinitrogen. Deuterated solvents were vacuum-transferred from CaH_2 ($CDCl_3$, CD_3CN). ^1H and ^{31}P NMR spectra were recorded on a Varian UNITY plus-500 spectrometer at ambient temperature unless otherwise noted. ^1H and $^{31}P\{^1H\}$ NMR chemical shifts are reported relative to undeuterated impurities of $CDCl_3$ or CD_3CN and external 85% H_3PO_4, respectively. Infrared spectra were recorded on a Perkin-Elmer 2000 FT-IR spectrometer. UV−vis spectra were measured using a JASCO V560 spectrometer. Mass spectra were collected on an API 300 triple quadruple LC/MS/MS mass spectrometer (Perkin-Elmer Sciex Instruments). Elemental analyses for C, H, N, and S were performed on a LECO-CHNS-932 elemental analyzer where the crystalline samples were sealed in thin silver tubes. The cyclic voltammogram of **5** was recorded in DMF on a glassy carbon electrode with Bu_4NClO_4 as the supporting electrolyte. The potentials are reported versus saturated calomel electrode, SCE. $(CH_3)_2PCH_2CH_2SH$ (Hdmsp),[12a] $Ph_2PCH_2CH_2SH$ (Hdpsp),[12b] $(PPh_4)[(EtS)W(S)_3]$,[8] and $[Fe(CH_3CN)_6][ClO_4]_2$[14] were prepared according to the literature methods.

Preparation of $(PPh_4)[(dmsp)W(S)_3]$ (1a). To a solution of $(PPh_4)[(EtS)W(S)_3]$ (0.43 g, 0.63 mmol) in THF (50 mL) was added Hdmsp (90 mg, 0.74 mmol). The mixture was stirred at room temperature for 3 h, during which time the color of the solution gradually changed from orange to red. After centrifugation to remove a small amount of insoluble materials, the solution was

(4) (a) Wieghardt, K.; Hahn, M.; Weiss, J.; Swiridoff, W. *Z. Anorg. Allg. Chem.* **1982**, *492*, 164−174. (b) Gheller, S. F.; Hambley, T. W.; Traill, P. R.; Brownlee, R. T. C.; O'Connor, M. J.; Snow, M. R.; Wedd, A. G. *Aust. J. Chem.* **1982**, *35*, 2183-2191. (c) Klingelhöfer, P.; Müller, U. *Z. Anorg. Allg. Chem.* **1988**, *556*, 70−78. (d) Faller, J. W.; Kucharczyk, R. R.; Ma, Y. *Inorg. Chem.* **1990**, *29*, 1662−1667. (e) Yoshida, T.; Adachi, T.; Matsumura, K.; Kawazu, K.; Baba, K. *Chem. Lett.* **1991**, 1067−1070. (f) Rabinovich, D.; Parkin, G. *J. Am. Chem. Soc.* **1991**, *113*, 5904−5905. (g) Eagle, A. A.; Harben, S. M.; Tiekink, E. R. T.; Young, C. G. *J. Am. Chem. Soc.* **1994**, *116*, 9749−9750. (h) Murphy, V. J.; Parkin, G. *J. Am. Chem. Soc.* **1995**, *117*, 3522−3528. (i) Rabinovich, D.; Parkin, G. *Inorg. Chem.* **1995**, *34*, 6341−6361. (j) Cotton, F. A.; Schmid, G. *Inorg. Chem.* **1997**, *36*, 2267−2278. (k) Miao, M.; Willer, M. W.; Holm, R. H. *Inorg. Chem.* **2000**, *39*, 2843−2849.

(5) Seino, H.; Arai, Y.; Iwata, N.; Nagao, S.; Mizobe, Y.; Hidai, M. *Inorg. Chem.* **2001**, *40*, 1677−1682.

(6) (a) Tatsumi, K.; Inoue, Y.; Nakamura, A.; Cramer, R. E.; VanDoorne, W.; Gilje, J. W. *J. Am. Chem. Soc.* **1989**, *111*, 782−783. (b) Tatsumi, K.; Inoue, Y.; Kawaguchi, H.; Kohasaka, M.; Nakamura, A.; Cramer, R. E.; VanDoorne, W.; Taogoshi, G. J.; Richmann, P. N. *Organometallics* **1993**, *12*, 352−364. (c) Kawaguchi, H.; Tatsumi, K. *J. Am. Chem. Soc.* **1995**, *117*, 3885−3886. (d) Kawaguchi, H.; Yamada, K.; Lang, J.-P.; Tatsumi, K. *J. Am. Chem. Soc.* **1997**, *119*, 10346−10358.

(7) (a) Tatsumi, K.; Kawaguchi, H.; Inoue, Y.; Nakamura, A.; Cramer, R. E.; Golen, J. A. *Angew. Chem., Int. Ed. Engl.* **1993**, *32*, 763−765. (b) Lang, J.-P.; Kawaguchi, H.; Ohnishi, S.; Tatsumi, K. *Chem. Commun.* **1997**, 405−406. (c) Lang, J.-P.; Kawaguchi, H.; Tatsumi, K. *Inorg. Chem.* **1997**, *36*, 6447−6449. (d) Lang, J.-P.; Tatsumi, K. *Inorg. Chem.* **1998**, *37*, 160−162. (e) Lang, J.-P.; Kawaguchi, H.; Ohnishi, S.; Tatsumi, K. *Inorg. Chim. Acta* **1998**, *283*, 136−144. (f) Lang, J.-P.; Kawaguchi, H.; Tatsumi, K. *J. Organomet. Chem.* **1998**, *569*, 109−119. (g) Lang, J.-P.; Tatsumi, K. *Inorg. Chem.* **1999**, *38*, 1364−1367. (h) Lang, J.-P.; Kawaguchi, H.; Tatsumi, K. *Chem. Commun.* **1999**, 2315−2316.

(8) (a) Boorman, P. M.; Wang, M.; Parvez, M. *J. Chem. Soc., Chem. Commun.* **1995**, 999−1000. (b) Kruhlak, N. L.; Wang, M.; Boorman, P. M.; Parvez, M.; McDonald, R. *Inorg. Chem.* **2001**, *40*, 3141−3148. (c) Boorman, P. M.; Gao, X.-L.; Kraatz, H. B.; Mozol, V.; Wang, M.-P. In *Tranistion Metal Sulfur Chemistry*; Stiefel, E. I., Matsumoto, K., Eds.; ACS Symposium Series 653; American Chemical Society: Washington, DC, 1996; pp 197−214.

(9) Lang, J.-P.; Kawaguchi, H.; Tatsumi, K. Submitted for publication.

(10) Coucouvanis, D.; Chen, S.-J.; Mandimutrira, B. S.; Kim, C. G. *Inorg. Chem.* **1994**, *33*, 4429−4430.

(11) Lang, J.-P.; Tatsumi, K. Unpublished result.

(12) (a) Kita, M.; Yamamoto, T.; Kashiwabara, K.; Fujita, J. *Bull. Chem. Soc. Jpn.* **1992**, *65*, 2272−2274. (b) Chatt, J.; Dilworth, J. R.; Schmutz, J. A.; Zubieta, J. A. *J. Chem. Soc., Dalton Trans.* **1979**, 1595−1599.

(13) Arikawa, Y.; Kawaguchi, H.; Kashiwabara, K.; Tatsumi, K. *Inorg. Chem.* **1999**, *38*, 4549−4553.

(14) West, R. J.; Lincoln, S. F. *Aust. J. Chem.* **1971**, *24*, 1169−1175.

cooled to −20 °C. Dark red crystals of **1a** were isolated in 97% yield (0.54 g). ^{1}H NMR (CD_3CN): δ 1.62 (d, 6H, P*Me*$_2$, J_{PH} = 10 Hz), 2.17 (dt, 2H, C*H*$_2$P, J_{PH} = 9.8 Hz, J_{HH} = 6.8 Hz), 3.04 (dt, 2H, SC*H*$_2$, J_{PH} = 16 Hz, J_{HH} = 6.8 Hz), 7.67−7.94 (m, 20H, PPh_4). ^{31}P{^{1}H} NMR (CD_3CN): δ 23.3 (s, J_{PW} = 83 Hz, dmsp), 24.3 (s, PPh_4). IR (KBr, pellet): 1584 (m), 1483 (m), 1436 (s), 1405 (w), 1290 (w), 1277 (m), 1107 (s), 996(m), 949 (m), 934 (s), 911 (s), 754 (m), 723 (s), 690 (s), 526 (s), 474 (m, $\nu_{W=S}$), 458 (s, $\nu_{W=S}$), 434 (s, $\nu_{W=S}$) cm^{-1}. UV−vis (λ_{max}, nm ($\epsilon \times 10^{-4}$, M^{-1} cm^{-1}), CH_3CN): 262 (1.1), 268 (1.2), 276 (1.1), 296 (0.87), 389 (0.43), 470 (0.34). MS (ESI-MS): *m*/*z* 401 (M^-). Anal. Calcd for $C_{36}H_{46}O_2P_2W_1S_4$: C, 48.87; H, 5.24; S, 14.50. Found: C, 48.38; H, 5.24; S, 14.37.

Preparation of (PPh_4)[(dpsp)W(S)$_3$] (1b). A THF (25 mL) solution of (PPh_4)[(EtS)W(S)$_3$] (0.23 g, 0.34 mmol) and Hdpsp (0.13 g, 0.53 mmol) was stirred overnight. Upon concentrating the solution in vacuo, the color turned red. Insoluble materials were removed by centrifugation, and the solution was cooled to −20 °C. Dark red crystals of **1b** were obtained (0.27 g, 85%). ^{1}H NMR (CD_3CN): δ 2.66 (dt, 2H, C*H*$_2$P, J_{PH} = 6.8 Hz, J_{HH} = 6.8 Hz), 2.92 (dt, 2H, SC*H*$_2$, J_{PH} = 15 Hz, J_{HH} = 6.8 Hz), 7.38−7.42 (m, 6H, PPh_2), 7.67−7.94 (m, 24H, PPh_2, and PPh_4). ^{31}P{^{1}H} NMR (CD_3CN): δ 18.8 (brs, $\Delta\nu_{1/2}$ = 41 Hz, dpsp), 24.3 (s, PPh_4). IR (KBr, pellet): 1584 (m), 1482 (m), 1434 (s), 1108 (s), 995 (m), 755 (m), 723 (s), 692 (s), 529 (s), 495 (m, $\nu_{W=S}$), 480 (m, $\nu_{W=S}$), 464 (s, $\nu_{W=S}$), 437 (s, $\nu_{W=S}$) cm^{-1}. UV−vis (λ_{max}, nm ($\epsilon \times 10^{-4}$, M^{-1} cm^{-1}), CH_3CN): 268 (2.1), 275 (1.9), 293 (1.5), 386 (0.68), 419 (sh), 473 (0.45). MS (ESI-MS): *m*/*z* 525 (M^-). Anal. Calcd for $C_{42}H_{42}O_1P_2W_1S_4$: C, 53.85; H, 4.52; S, 13.69. Found: C, 53.52; H, 4.61; S, 13.91.

Synthesis of (dmsp)WS$_3$Cu$_2$(PPh$_3$)$_2$Br (2). To a solution of **1a** (0.12 g, 0.16 mmol) in CH_3CN (15 mL) was added CuBr (47 mg, 0.33 mmol) in CH_3CN (15 mL). The red solution immediately darkened. The mixture was stirred overnight at room temperature. After centrifugation to remove insoluble materials, PPh_3 (86 mg, 0.33 mmol) was added to the supernatant. Upon stirring the solution for 4 h, dark red microcrystals precipitated, which were collected by decantation. Recrystallization from warm CH_3CN yielded **2** as dark red crystals (0.18 g, 96%). ^{1}H NMR ($CDCl_3$): δ 2.19 (d, 6H, P*Me*$_2$, J_{PH} = 10 Hz), 2.37−2.42 (m, 2H, C*H*$_2$P), 3.30 (dt, 2H, SC*H*$_2$, J_{PH} = 18 Hz, J_{HH} = 6.6 Hz), 7.30−7.62 (m, 30H, PPh_3). ^{31}P{^{1}H} NMR ($CDCl_3$): δ 12.6 (br, $\Delta\nu_{1/2}$ = 170 Hz, PPh_3), 43.4 (s, J_{PW} = 150 Hz, dmsp). IR (KBr, pellet): 1480 (s), 1436 (vs), 1097 (s), 1027 (m), 997(m), 950, (m), 933 (m), 911 (m), 744 (s), 694 (vs), 520 (s), 505 (s), 494 (m) cm^{-1}. Anal. Calcd for $C_{42}H_{43}Br_1Cu_2N_1P_3W_1S_4$: C, 42.98; H, 3.69; N, 1.19; S, 10.93. Found: C, 43.01; H, 3.80; N, 1.31; S, 11.18.

Preparation of (PPh_4)[(dmsp)WS$_3$(FeCl$_2$)] (3). Addition of $FeCl_2$ (17 mg, 0.13 mmol) in CH_3CN (10 mL) to (PPh_4)[(dmsp)W(S)$_3$] (**1a**) (90 mg, 0.12 mmol) in CH_3CN (5 mL) immediately gave a dark red solution. After stirring at room temperature for 3 h, the mixture was centrifuged to remove an insoluble solid. The solution was concentrated, and Et_2O was layered to form a red brown crystalline powder of **3** (70 mg, 67%). Recrystallization from CH_3CN/Et_2O afforded **3** as dark red needles. IR (KBr, pellet): 1586 (m), 1481 (m), 1435 (s), 1419 (w), 1411 (w), 1340 (w), 1286 (m), 1109 (s), 954 (s), 933 (s), 911 (s), 996 (m), 759 (s), 724 (s), 690 (s), 528 (s), 513 (s, $\nu_{W=S}$), 467 (m), 457 (m), 430 (s), 410 (s) cm^{-1}. UV−vis (λ_{max}, nm ($\epsilon \times 10^{-4}$, M^{-1} cm^{-1}), CH_3CN): 269 (1.7), 276 (1.6), 291 (1.4), 424 (0.31). MS (ESI-MS): *m*/*z* 529 (M^-). X-ray fluorescence microanalysis: W/Fe/Cl/S/P = 1.00/1.12/2.16/3.89/2.23. Anal. Calcd for $C_{28}H_{30}P_2S_4W_1Fe_1Cl_2$: C, 38.77; H, 3.49; S, 14.79. Found: C, 38.15; H, 3.42; S, 14.55.

Synthesis of [(dmsp)WS$_3$]$_2$Fe$_2$Cl (4). To a solution of **3** (0.32 g, 0.37 mmol) in CH_3CN (30 mL) was added $[Fe(CH_3CN)_6][ClO_4]_2$ (0.21 g, 0.41 mmol) in CH_3CN (2 mL). The red-brown solution was stirred overnaight at room temperature and was concentrated. A crude product contaminated by colorless $(PPh_4)(ClO_4)$ was washed with CH_3CN (10 mL × 3) and dried in vacuo, leaving **4** as a dark brown powder (80 mg, 46%). Crystallization from CH_3CN/Et_2O gave dark brown crystals of **4**. IR (KBr, pellet): 1408 (m), 1248 (m), 951, (m), 933 (s), 916 (m), 521 (m), 445 (m) cm^{-1}. X-ray fluorescence microanalysis: W/Fe/Cl/S/P = 1.00/0.95/0.46/4.12/1.17. Anal. Calcd for $C_8H_{20}P_2W_2S_8Fe_2Cl_1$: C, 10.12; H, 2.12; S, 27.02. Found: C,10.93; H, 2.32; S, 26.92.

Synthesis of [(dmsp)WS$_3$Fe]$_4$ (5). Addition of $[Fe(CH_3CN)_6][ClO_4]_2$ (0.26 g, 0.52 mmol) in CH_3CN (15 mL) to a CH_3CN (15 mL) solution of (PPh_4)[(dmsp)W(S)$_3$] (**1a**) (0.19 g, 0.26 mmol) caused immediate precipitaion of a dark brown solid. A workup analogous to that for **4** led to isolation of **5** as a dark brown powder (60 mg, 50%). Recrystallization from DMF afforded black crystals of **5**. IR (KBr, pellet): 1405 (m), 1284 (m), 949, (s), 933 (s), 911 (s), 448 (m), 442 (m), 421 (m), 411 (m) cm^{-1}. X-ray fluorescence microanalysis: W/Fe/S/P = 1.00/0.73/3.98/0.97. Anal. Calcd for $C_{16}H_{40}P_4W_4S_{16}Fe_4$: C, 10.51; H, 2.21; S, 28.06. Found: C,10.49; H, 2.31; S, 28.25.

X-ray Crystal Structure Determinations. Crystallographic data are summarized in Table 1. X-ray quality single crystals of **1a**·2THF and **1b**·THF were obtained by recrystallization from THF, while those of **2**·CH_3CN and **5**·4DMF were obtained from CH_3CN and DMF, respectively. Crystals of **3** and **4** were grown by slow diffusion of Et_2O into their CH_3CN solutions. Diffraction data were collected on a Rigaku-AFC7 equipped with a MSC/ADSC Quantum1 CCD area detector. The measurements were made by using graphite monochromated Mo Kα radiation (λ = 0.710 69 Å) at 173 K under a cold nitrogen stream for **1**−**4** and at room temperature for **5**. Single crystals of **1**−**4** were mounted at the top of quartz fibers using Paratone-N, and the crystal of **5** was sealed in a glass capillary under argon. The intensity images were obtained with ω scans of 0.5° interval per frame for duration of 81 s (**1a**) or 175 s (**3** and **5**) for each frame, and 0.3° intervals of ω for 44 s each (**1b**, **2**, and **4**). The frame data were processed using a d*TREK program package, and the reflection data were corrected for absorption with a REQAB program.

All calculations were performed with a TEXSAN package. The structures were solved by direct methods, which showed the metal atom positions unequivocally. The other heavy atoms were found in subsequent Fourier maps, and the structures were refined by full-matrix least squares. All non-hydrogen atoms were refined anisotropically, except for DMF molecules of **5**. Refinement of individual atom positions of DMF was not successful, and each DMF was treated as a rigid group with isotropic thermal parameters. The hydrogen atoms were put at calculated positions with C−H distances of 0.97 Å, while hydrogen atoms of THF in **1a**·2THF were not included in the calculations. Additional crystallographic data are given in Supporting Information.

Results and Discussion

Synthesis of (PPh_4)[(L)W(S)$_3$] (L = dmsp (1a), dpsp (1b)). Our strategy for preparation of the trithiotungsten complexes having phosphine-thiolate hybrid ligands was to employ ligand exchange reactions of the previously described trithio complex (PPh_4)[(EtS)W(S)$_3$] with appropriate phosphine-thiols (Scheme 1). The reaction with Hdmsp went smoothly in THF at room temperature with a gradual color

Table 1. Crystal Data for $(PPh_4)[(dmsp)W(S)_3]$ (**1a**), $(PPh_4)[(dpsp)W(S)_3]$ (**1b**), $(dmsp)WS_3Cu_2(PPh_3)_2Br$ (**2**), $(PPh_4)[(dmsp)WS_3(FeCl_2)]$ (**3**), $[(dmsp)WS_3]_2Fe_2Cl$ (**4**), and $[(dmsp)WS_3Fe]_4$ (**5**)

	1a·2THF	**1b**·THF	**2**·CH_3CN	**3**	**4**	**5**·4DMF
formula	$C_{36}H_{46}O_2S_4P_2W$	$C_{42}H_{42}OS_4P_2W$	$C_{42}H_{43}NS_4P_3BrWCu_2$	$C_{28}H_{30}S_4P_2Cl_2WFe$	$C_8H_{20}S_8P_2ClW_2Fe_2$	$C_{28}H_{40}N_4O_4S_{16}P_4W_4Fe_4$
mol wt (g mol^{-1})	868.67	936.83	1173.82	867.34	949.52	2092.29
cryst syst	orthorhombic	triclinic	monoclinic	orthorhombic	tetragonal	triclinic
space group	*Pna2$_1$* (No. 33)	*P*−*1* (No. 2)	*P2$_1$/c* (No. 14)	*P2$_1$2$_1$2$_1$* (No. 19)	*I4$_1$/a* (No. 88)	*P*−*1* (No. 2)
cryst color	dark red	dark red	dark red	dark red	dark brown	black
cryst size (mm^3)	0.20 × 0.10 × 0.05	0.30 × 0.10 × 0.05	0.25 × 0.20 × 0.10	0.25 × 0.05 × 0.05	0.15 × 0.10 × 0.10	0.20 × 0.20 × 0.10
a (Å)	22.524(1)	11.034(3)	17.845(1)	9.3708(5)	13.0303(3)	14.994(2)
b (Å)	9.1893(3)	11.172(2)	10.0916(1)	17.3605(5)		13.515(1)
c (Å)	18.2715(3)	18.354(4)	25.6060(6)	20.246(1)	29.5638(9)	17.812(3)
α (deg)		80.070(2)				80.655(2)
β (deg)		76.363(2)	101.7941(7)			99.003(1)
γ (deg)		63.973(2)				113.025(2)
V (Å^3)	3781.8(4)	1969.5(6)	4513.9(2)	3293.7(2)	5019.6(2)	3260.6(6)
Z	4	2	4	4	8	2
ρ_{calcd} (g cm^{-3})	1.526	1.580	1.727	1.749	2.513	2.131
$2\theta_{max}$ (deg)	55.1	55.0	55.6	55.4	55.0	55.2
no. unique rflns	4666	8343	9862	4108	2919	13748
no. obsd rflns [a]	3683	6676	6519	2780	2043	4516
no. params	406	451	487	343	110	425
R[b]	0.036	0.060	0.040	0.064	0.065	0.048
R_w[c]	0.045	0.071	0.049	0.075	0.073	0.053
GOF[d]	1.13	2.05	1.59	1.53	2.50	1.69

[a] Observation criterion $I > 3\sigma(I)$. [b] $R = \sum||F_o| - |F_c||/\sum|F_o|$. [c] $R_w = \{\sum w(|F_o| - |F_c|)^2/\sum wF_o^2\}^{1/2}$. [d] GOF $= [\{\sum w(|F_o| - |F_c|)^2\}/(N_o - N_p)]^{1/2}$, where N_o and N_p denote the number of data and parameters.

Scheme 1

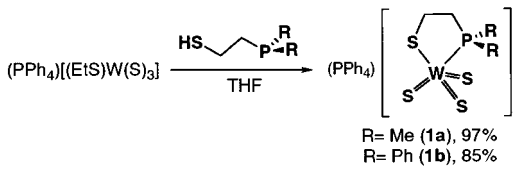

change from orange to red. Upon standing the solution at −20 °C, dark red crystals were formed, and the desired complex $(PPh_4)[(dmsp)W(S)_3]$ (**1a**) was isolated in 97% yield. The analogous reaction with Hdpsp proceeded very slowly, and the color change was noticed when the THF solution was concentrated in vacuo. Volatile substances were removed under vacuum, and the subsequent standard workup led to isolation of $(PPh_4)[(dpsp)W(S)_3]$ (**1b**) in 85% yield as dark red crystals. Removal of ethanethiol from the reaction system appears to be essential for the formation of **1b**, indicating that coordination of dpsp at W is less favorable than that of ethanethiolate.

The elemental analysis and ^1H NMR spectra in CD_3CN of **1a** and **1b** are consistent with their formulation. The $^{31}P\{^1H\}$ NMR spectra of **1a** show a signal at δ 23.3 with ^{183}W satellites ($J_{W-P} = 83$ Hz) assignable to the coordinated phosphorus atom of dmsp, which is substantially shifted downfield compared with the peak (δ −51.3) of free Hdmsp. For **1b**, the $^{31}P\{^1H\}$ NMR signal of dpsp appears as a broad peak at δ 18.8 ($\Delta\nu_{1/2} = 41$ Hz), and ^{183}W satellites were not clearly seen. Again, this dpsp signal is shifted downfield relative to free Hdpsp (δ −17.6), but to a lesser extent than the dmsp signal of **1a**. The P−W coordination bond of **1b** may be partially dissociated in solution, while the phosphine portion of dmsp of **1a** is tightly bound to W. The IR spectra in the solid are featured by relatively strong W═S stretching bands in the 430−500 cm^{-1} region, appearing at 434, 458, and 474 cm^{-1} for **1a** and at 437, 464, 480, and 495 cm^{-1} for **1b**. These bands are at lower frequencies than the corresponding bands of $(PPh_4)[(EtS)W(S)_3]$ (482, 494, and 504 cm^{-1}). Additional coordination by the phosphine portion of dmsp or dpsp is probably a reason for the shift of the W═S stretching bands. The W═S stretching frequencies of $(PPh_4)[Cp^*W(S)_3]$ (437, 466 cm^{-1})[6c] are similar to those of **1a** and **1b**.

The X-ray structure of the anionic part of **1a** is shown in Figure 1. The structure of **1b** is similar to that of **1a**, and the bond distances and angles of the two complexes are compared in Table 2. The coordination geometry at W is best described as a distorted trigonal bipyramid, where P1 and S3 occupy the axial positions. The S3−W−P1 bonds deviate from linearity by 23.26(8)° and 20.87(8)° for **1a** and **1b**, respectively, and the W atoms move out from the equatorial S1S2S4 planes toward S3 by 0.32 and 0.35 Å. For either **1a** or **1b**, the axial W═S3 bond is elongated because of the trans influence of phosphine coordination. The equatorial W═S2 bond is also long, because the

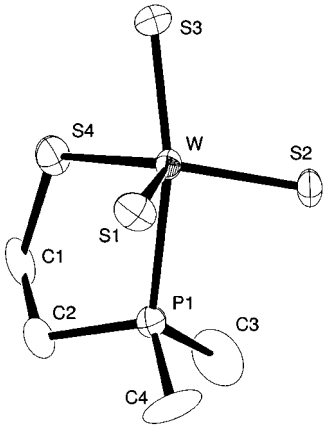

Figure 1. ORTEP drawing of the complex anion of $(PPh_4)[(dmsp)W(S)_3]$, **1a**, including non-hydrogen atom numbering. Here and in the following figures, non-hydrogen atoms are represented by 50% probability thermal ellipsoids, and hydrogen atoms are omitted for clarity.

Table 2. Selected Bond Distances (Å) and Angles (deg) for $(PPh_4)[(dmsp)W(S)_3]$ (**1a**) and $(PPh_4)[(dpsp)W(S)_3]$ (**1b**)

	1a	**1b**
	Bond Distances (Å)	
W−S1	2.132(2)	2.164(2)
W−S2	2.214(2)	2.190(2)
W−S3	2.221(2)	2.223(2)
W−S4	2.425(2)	2.407(2)
W−P1	2.572(2)	2.587(2)
	Bond Angles (deg)	
S1−W−S2	110.5(1)	110.83(9)
S1−W−S3	109.05(8)	108.03(9)
S2−W−S3	105.33(8)	106.23(8)
S2−W−S4	125.27(8)	125.46(8)
S1−W−S4	118.11(8)	116.59(9)
S3−W−P1	156.74(8)	159.13(8)

substantially larger S4−W−S2 angle, relative to S4−W−S1, exerts the trans influence of S4 more effectively to this bond. Consequently, the average W═S distances of **1a** (2.189 Å) and **1b** (2.192 Å) are longer than those of $(PPh_4)[(EtS)W(S)_3]$ (2.154 Å)[8a] and $(NH_4)_2[W(S)_4]$ (2.177 Å),[2a] while they are comparable to the W═S bonds of $(PPh_4)[Cp^*W(S)_3]$ (2.192 Å).[6d] This observation is consistent with the trend of W═S stretching bands of these trithio complexes. The bond distances between tungsten and the thiolate sulfurs (S4) of dmsp and dpsp are substantially longer than the W−SEt bond of $(PPh_4)[(EtS)W(S)_3]$ (2.323(3) Å).[8a] Interestingly, the W−P1 distance of **1b** is slightly longer than that of **1a**, while the W−S4 bond is shorter for **1b**. This geometrical trend accounts for lability of the dpsp ligand in solution, which was indicated by the $^{31}P\{^1H\}$ NMR spectra. The bulk of phenyl groups at phosphorus of **1b** may be a reason for the elongation of W−P1 bond, and/or the strong donor ability of methyl groups could strengthen the bond for **1a**.

Cluster Forming Reactions of $(PPh_4)[(dmsp)W(S)_3]$ (1a). As described earlier in this paper, trithio(thiolato) complexes of tungsten, $(PPh_4)[(RS)W(S)_3]$, tend to degrade in solution via complicated ligand exchange and/or redox reactions. Addition of donor ligands such as PPh_3 and pyridine to a solution of $(PPh_4)[(EtS)W(S)_3]$ did not aid in stabilization of the complex. On the other hand, **1a** and **1b** were found to be stable at room temperature for a prolonged period in CD_3CN, according to the ^1H NMR spectra.

Scheme 2

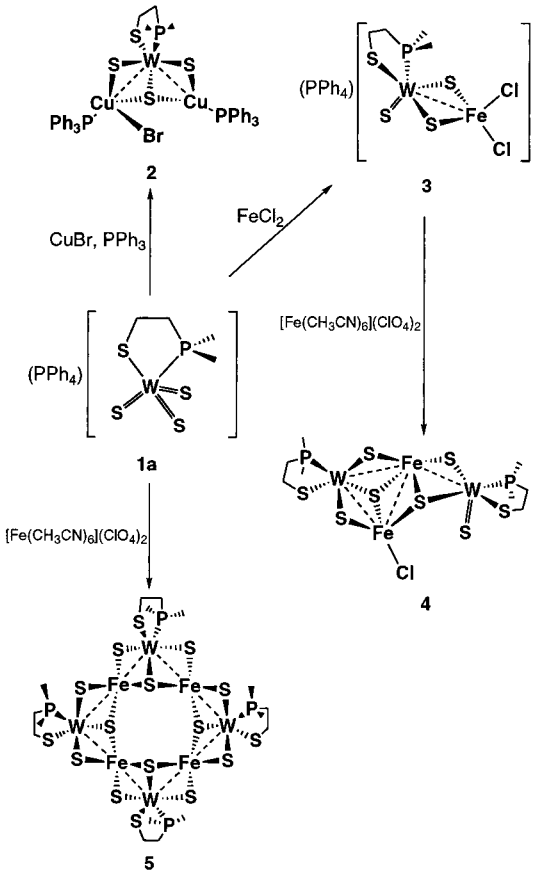

Additional coordination of the dmsp (or dpsp) phosphine must be a reason for the increase in stability, by preventing the degradation processes arising from coordinative unsaturation of trithio(thiolato) complexes. Encouraged by this observation, we carried out cluster forming reactions of **1a** with CuBr, $FeCl_2$, and $[Fe(CH_3CN)_6](ClO_4)_2$. The results are summarized in Scheme 2, and the details are given in the following paragraphs.

(a) Reaction with CuBr. When 2 equiv of CuBr was added to a red solution of **1a** in CH_3CN, the color immediately darkened. The mixture was allowed to stir at room temperature overnight, and addition of PPh_3 to the solution resulted in the precipitation of dark red crystals. The X-ray study of the red crystal shows that the product is $(dmsp)WS_3Cu_2(PPh_3)_2Br$ (**2**) (96% yield), and the spectroscopic data and the elemental analysis were consistent with the formulation. On the other hand, isolation of products from the reaction system without PPh_3 has not been successful.

The molecular structure of **2** is shown in Figure 2, and the selected bond distances and angles are listed in Table 3. The cluster consists of a WS_3Cu_2Br core, where the copper atoms are each bound to one triphenylphosphine and two terminal sulfides of $[(dmsp)W(S)_3]^-$. Although the Br atom bestrides over Cu1 and Cu2, the Cu1−Br distance is much shorter than Cu2−Br (2.961(1) Å). The bonding interaction between Cu2 and Br must be very weak, if there is any. Consequently, Cu1 adopts a tetrahedral geometry, while the coordination geometry of Cu2 is regarded as trigonal planar where Cu2 moves off the S2S3P3 plane by 0.33 Å. The

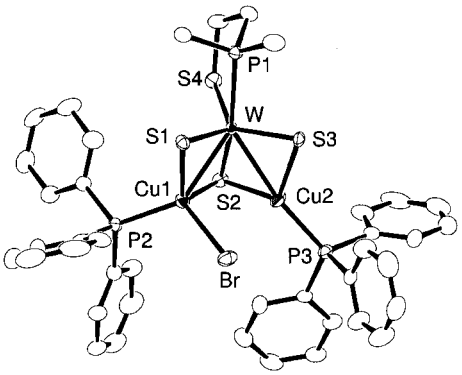

Figure 2. ORTEP drawing of $(dmsp)WS_3Cu_2(PPh_3)_2Br$, **2**.

Table 3. Selected Bond Distances (Å) and Angles (deg) in $(dmsp)WS_3Cu_2(PPh_3)_2Br$ (**2**)

Bond Distances (Å)			
W−Cu1	2.6808(9)	W−Cu2	2.6323(9)
W−S1	2.206(2)	W−S2	2.331(2)
W−S3	2.220(2)	W−S4	2.370(2)
W−P1	2.543(2)	Br−Cu1	2.519(1)
Bond Angles (deg)			
Cu1−W−Cu2	68.36(3)	W−Cu1−Br	107.12(4)
S1−W−S2	106.60(7)	S1−W−S3	111.49(6)
S1−W−S4	120.31(6)	S1−W−P1	84.80(6)
S2−W−S3	105.54(6)	S2−W−S4	80.19(6)
S2−W−P1	157.45(6)	S3−W−S4	123.72(6)
S3−W−P1	87.42(6)	S4−W−P1	77.26(6)

W−Cu distances are comparable to those of the known W/Cu/S clusters,[7e,f,15] where dative bonding between d^{10} Cu(I) and d^0 W(VI) was suggested. The different coordination numbers of Cu1 and Cu2 cause a slight variation of the W−Cu bond distances. The metal−metal bond is elongated by 0.0485(9) Å for the four coordinated copper, namely Cu1. The tungsten atom retains the trigonal bipyramidal geometry of **1a**, in which the axial positions are occupied by P1 (dmsp) and μ_3-S2. Actually, the coordination geometry at W for **2** is even closer to the ideal trigonal prism, in that the equatorial S−W−S angles do not deviate much from 120° and in that the out-of-plane displacement of W is smaller (0.35 Å). Because S2 bridges three metal atoms, the W−S2 distance is long. On the other hand, the W−S4 and W−P bonds are somewhat shortened compared with those of **1a**, because coordination of Cu atoms weakened the multiple W═S bonds, which is compensated by stronger W−dmsp interactions.

Although the molecular structure of **2** is unsymmetric in crystals, the methyl proton signal of dmsp appears as a sharp doublet (J_{PH} = 10 Hz) in the ^{1}H NMR spectrum even at −30 °C. Thus, the cluster structure is fluxional in solution via a dynamic process involving a fast exchange of the Br coordination site between two Cu centers. The $^{31}P\{^1H\}$ NMR spectrum exhibits a broad peak of PPh_3 at δ 12.6, in addition to the dmsp signal. The broadening is due to the coupling between the ^{31}P and ^{63}Cu (^{65}Cu) nuclei. The phosphorus peak of dmsp is shifted further downfield (δ 43.3) from that of

(15) (a) Müller, A.; Bögge, H.; Schimanski, U.; Penk, M.; Nieradzik, K.; Dartmann, M.; Krickemeyer, E.; Schimanski, J.; Romer, C.; Romer, M.; Dornfeld, H.; Wienboker, U.; Hellmann, W.; Zimmermann, M. *Monatsh. Chem.* **1989**, *120*, 367−391. (b) Lang, J.; Tatsumi, K. *J. Organomet. Chem.* **1999**, *579*, 332−337.

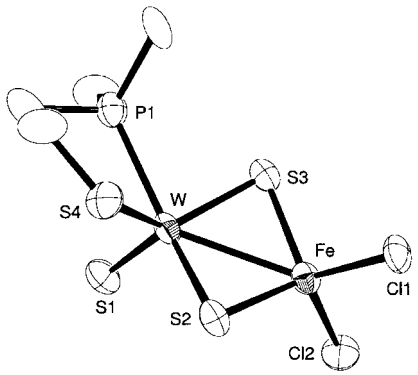

Figure 3. ORTEP drawing of the complex anion of $(PPh_4)[(dmsp)WS_3(FeCl_2)]$, **3**.

Table 4. Selected Bond Distances (Å) and Angles (deg) in $(PPh_4)[(dmsp)WS_3(FeCl_2)]$ (**3**)

Bond Distances (Å)			
W−Fe	2.756(3)	W−S1	2.141(5)
W−S2	2.314(7)	W−S3	2.260(5)
W−S4	2.382(6)	W−P1	2.532(6)
Fe−S2	2.257(6)	Fe−S3	2.278(7)
Fe−Cl1	2.247(6)	Fe−Cl2	2.264(6)
Bond Angles (deg)			
S1−W−S2	107.7(2)	S1−W−S3	111.3(2)
S1−W−S4	114.6(2)	S1−W−P1	89.4(2)
S2−W−S3	103.6(2)	S2−W−S4	82.9(2)
S2−W−P1	158.2(2)	S3−W−S4	128.9(2)
S3−W−P1	81.7(2)	S4−W−P1	77.6(2)

1a and also shows ^{183}W satellites with a larger W−P coupling constant of 150 Hz. The downfield shift and larger J_{W-P} value, relative to those of **1a**, may arise from the shorter W−P bond length. The IR spectrum of **2** does not show a band arising from W═S stretching, because the terminal sulfides coordinate to Cu atoms.

(b) Synthesis of Fe/W/S Clusters. Treatment of **1a** with 1 equiv of $FeCl_2$ in CH_3CN gave a dark red solution, from which we isolated $(PPh_4)[(dmsp)WS_3(FeCl_2)]$ (**3**) as dark red needles in 67% yield. The ^{1}H NMR spectrum of **3** is not informative because of its paramagnetic nature, while a strong absorption at 513 cm^{-1} in the IR spectrum indicates the presence of a terminal W═S bond. The negative ESI mass spectrum in CH_3CN clearly shows a set of peaks associated with the parent molecular ion $[(dmsp)WS_3(FeCl_2)]^-$. The observed isotopic pattern matches very well with the theoretical isotopic distribution. The elemental analysis and the X-ray fluorescence microanalysis are also consistent with the formation of a 1:1 adduct of $(PPh_4)[(dmsp)W(S)_3]$ and $FeCl_2$.

The X-ray analysis of **3** in fact shows that one $FeCl_2$ unit is bound to $[(dmsp)W(S)_3]^-$, where the Fe atom bridges two sulfides, namely S2 and S3, as shown in Figure 3. The selected geometrical parameters are given in Table 4. The trigonal bipyramid geometry at tungsten is again retained, and P1 and S2 occupy the axial positions, while geometry at Fe is tetrahedral. Coordination of two terminal sulfides to Fe weakens the W═S bonds, which in turn shortens the W−dmsp bond compared with the structure of **1a**. The situation is very similar to the strengthening of the W−dmsp bond of **2**, upon coordination of the sulfides to Cu atoms. As the WS_2Fe quadrilateral is folded by 19.7° along the S−S

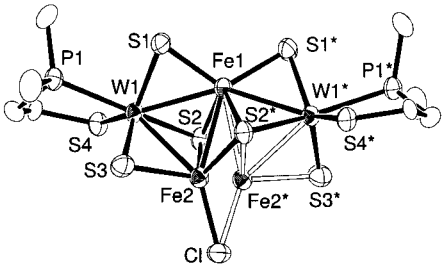

Figure 4. ORTEP drawing of $[(dmsp)WS_3]_2Fe_2Cl$, **4**. A crystallographic 2-fold axis runs through Fe1 and Cl, and the disordered Fe2 atom positions are superimposed.

Table 5. Selected Bond Distances (Å) and Angles (deg) in $[(dmsp)WS_3]_2Fe_2Cl$ (**4**)

Bond Distances (Å)			
W1−Fe1	2.6378(9)	W1−Fe2	2.694(4)
W1−S1	2.256(4)	W1−S2	2.376(4)
W1−S3	2.173(4)	W1−S4	2.362(3)
W1−P1	2.506(4)	Fe1−Fe2	2.644(5)
Fe2−Cl	2.215(6)		
Bond Angles (deg)			
W1−Fe1−W1*	147.2(1)	Fe1−W1−Fe2	59.4(1)
W1−Fe1−Fe2	61.34(9)	W1−Fe2−Fe1	59.22(8)
S1−W1−S2	101.7(1)	S1−W1−S3	112.5(2)
S2−W1−S3	106.8(1)	S2−W1−P1	157.5(1)

vector, the W−Fe distance of 2.756(3) Å is shorter than those of the closely related complexes, $(PPh_4)_2[WS_4(FeCl_2)]$ (2.794 Å)[8a] and $(PPh_4)[Cp^*WS_3(FeCl_2)]$ (2.795 Å).[9] The W−S2 bond is elongated because of the trans influence of P1, and the bond length is 0.05 Å longer than W−S3.

It was found that complex **3** did not react further with excess $FeCl_2$ and that **3** was the sole product even when **1a** was treated with 2 equiv of $FeCl_2$. Thus, $[(dmsp)W(S)_3]^-$ is not able to accommodate two $FeCl_2$ units. We then attempted to react **3** with a more labile Fe(II) ion source, $[Fe(CH_3CN)_6](ClO_4)_2$. From this **3**/$[Fe(CH_3CN)_6](ClO_4)_2$ (1:1) reaction system in CH_3CN were isolated dark brown crystals. On the basis of the X-ray study, the product was found to be a neutral W_2Fe_2 cluster formulated as $[(dmsp)WS_3]_2Fe_2Cl$ (**4**) (67% yield), and the elemental analysis and X-ray fluorescence microanalysis corroborated this formulation. In the crystal structure, an asymmetric unit contains a half portion of the molecule, and a crystallographic 2-fold axis runs through Fe1 and Cl atoms. The symmetry operation puts Fe2* at the position very near to Fe2. The very short Fe2−Fe2* separation of 1.316(8) Å suggests that the Fe2 atom is disordered over the two positions. As a matter of fact, the occupancy factor of Fe2 was estimated to be 50%. There was no short contact between molecules in the crystal. An ORTEP view of **4** is given in Figure 4, where the disordered Fe2 positions are superimposed. The selected bond distances and angles are listed in Table 5.

Cluster **4** consists of two $(dmsp)W(S)_3$ units, which are linked by two iron atoms. Once again, the coordination geometry at tungsten can be viewed as a trigonal bipyramid, and each iron assumes a tetrahedral geometry. An interesting facet of the structure is that two irons are not equivalent. The Fe1 atom links $(dmsp)W(S)_3$ units symmetrically, being surrounded by four sulfurs, while Fe2 is coordinated by three sulfurs and one chlorine. The average W−Fe distance of

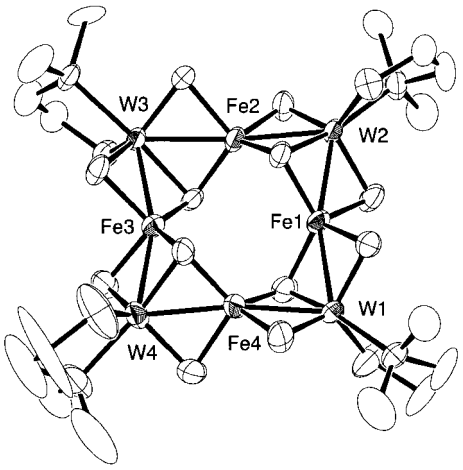

Figure 5. ORTEP drawing of $[(dmsp)WS_3Fe]_4$, **5**.

Table 6. Selected Bond Distances (Å) and Angles (deg) in $[(dmsp)WS_3Fe]_4$ (**5**)

Bond Distances (Å)			
W−Fe (av)	2.730		
W−μ_2-S (av)	2.217	W−μ_3-S (av)	2.375
W−S(dmsp) (av)	2.332	W−P (av)	2.515
Fe−μ_2-S (av)	2.251	Fe−μ_3-S (av)	2.258
Bond Angles (deg)			
Fe1−W1−Fe4	77.5(1)	Fe1−W2−Fe2	77.5(1)
Fe2−W3−Fe3	77.3(1)	Fe3−W4−Fe4	76.3(1)
W1−Fe1−W2	163.0(2)	W2−Fe2−W3	173.4(1)
W3−Fe3−W4	160.4(2)	W1−Fe4−W4	171.1(2)
μ_2-S−W−μ_2-S (av)	110.9	μ_2-S−W−μ_3-S (av)	104.5
S−Fe−S (av)	109.0		

2.666 Å is 0.09 Å shorter than the W−Fe bond of **3**, and the short Fe−Fe distance of 2.644(5) Å also suggests metal−metal bonding. Although it is not clear at the moment whether the iron atoms originate from $FeCl_2$ in **3** or from $[Fe(CH_3CN)_6](ClO_4)_2$, the presence of one chlorine atom in **4** leads to an enigmatic set of oxidation states of the metal ions. If the W(VI) oxidation state is retained, those of two iron atoms would formally be assigned as Fe(I) and Fe(II). Alternatively, if the oxidation state of two tungsten atoms is regarded as W(V), the iron atoms would be Fe(II) and Fe(III), or another possibility may be W(VI)−Fe(II)−Fe(II)−W(V). In either case, reduction of a metal center must have occurred. Thus, the formation of W_2Fe_2 cluster **4** involves a complicated redox process coupled with dissociation of chloride anion. A disproportionation reaction of $[Fe(CH_3CN)_6](ClO_4)_2$ might have taken place, which could be a cause for this reduction.

Finally, we examined the reaction of $(PPh_4)[(dmsp)W(S)_3]$ (**1a**) with $[Fe(CH_3CN)_6](ClO_4)_2$. This reaction in CH_3CN proceeded smoothly, and a dark brown powder was isolated in 50% yield. Recrystallization from DMF gave black crystals, the X-ray diffraction study of which revealed an cyclic octanuclear structure of $[(dmsp)WS_3Fe]_4$ (**5**), as shown in Figure 5. The important geometric parameters are listed in Table 6. The ^1H and $^{31}P\{^1H\}$ NMR spectra do not have assignable signals because of the paramagnetism of **5**, while the elemental analysis and X-ray fluorescence microanalysis support the formulation. The IR spectrum indicates that there is no W=S multiple bond.

The octanuclear cluster, **5**, consists of four (dmsp)$W(S)_3$ units and four Fe atoms, and the metal atoms form a square core. The metal atoms are arranged in such a way that four tungsten atoms occupy the corners of the square and four iron atoms reside in the edges. This W_4Fe_4 core is nearly planar, where the maximum deviation from the least-squared plane is 0.06 Å. The W−Fe−W bonds are slightly bent, because each Fe atom moves inward from the midpoint of an edge of the W_4 square. Coordination of dmsp occurs alternatively above and below the W_4Fe_4 plane, so that the cluster molecule has an approximate S_4 symmetry. All the sulfur atoms interact with Fe, resulting in four μ_3-S bridges and eight μ_2-S bridges. The absence of a W═S multiple bond is consistent with the IR spectrum. Each tungsten adopts a trigonal bipyramid geometry with P and μ_3-S at the axial positions, and the geometry at iron is tetrahedral. The average W−Fe distance of 2.730 Å is comparable to the W−Fe bond of **3**, while the long Fe−Fe separation of 3.41 Å excludes metal−metal bonding. The average W−μ_2-S and W−μ_3-S distances of 2.217 and 2.375 Å are similar to the corresponding bond distances of **2**, and the Fe−S distances are normal. The cyclic octanuclear structure of **5** resembles those of $[Cp^*WS_3Cu]_4$[15b] and $(Et_4N)_4[MOS_3Cu]_4$ (M = Mo, W),[16] in which four Cp^*WS_3 (or MOS_3) moieties are linked by four Cu atoms via sulfur bridges.

During the formation of **5**, acetonitrile molecules of $[Fe(CH_3CN)_6](ClO_4)_2$ are completely lost, and at the same time, a redox process took place to reduce metal centers. Although there is uncertainty in defining metal oxidation states, a plausible assignment would be W(VI) and Fe(I). In the closely related clusters, $[Cp^*WS_3Cu]_4$ and $(Et_4N)_4[WOS_3Cu]_4$, which are diamagnetic, the oxidation state of copper is best described as Cu(I), and that of tungsten is W(VI). The paramagnetism of **5** is likely to arise from the Fe(I) centers. We again think that a disproportionation reaction of $[Fe(CH_3CN)_6](ClO_4)_2$ caused the reduction. On the other hand, the cyclic voltammogram of **5** is featured by one reversible redox couple at 0.08 V ($E_{1/2}$ vs SCE) and three irreversible reduction steps at −1.29, −1.68, and −1.88 V (E_p vs SCE). The lack of multiple oxidation steps, which could occur at four Fe(I) sites, indicates that the reduced nature of Fe(I) may be dispersed over W(VI) sites.

Concluding Remark

It is known that thiolate sulfurs are capable of bridging metal centers. In fact, the dmsp sulfur of $Mo(dmsp)_2(S^tBu)_2$ plays an important role in the cluster forming reactions with $FeCl_2$ and CuBr to give $[Mo(O)(dmsp)_2]_2FeCl_2$ and $[MoBr(dmsp)_2(\mu_3\text{-}S)Cu_2]_2(\mu_2\text{-}S^tBu)_2$. In contrast, the dmsp ligand of $(PPh_4)[(dmsp)W(S)_3]$ (**1a**) remains intact during the reactions with $FeCl_2$, CuBr, and $[Fe(CH_3CN)_6](ClO_4)_2$. As a building block of sulfide clusters, **1a** behaves more like $[Cp^*W(S)_3]^-$ rather than $Mo(dmsp)_2(S^tBu)_2$, in that three terminal sulfides are bound to incoming metal fragments. The reaction of $(PPh_4)[Cp^*W(S)_3]$ in $CHCl_3$ with CuBr and PPh_3 gave $(PPh_4)[Cp^*WS_3Cu_2Br(PPh_3)_2]$,[15b] the main framework of which is very similar to **2** except that the Br atom bridges Cu atoms symmetrically. Also, the 1:1 adduct of $(PPh_4)[Cp^*W(S)_3]$ and $FeCl_2$ was readily formed in CH_3CN, and its structure is analogous to that of **3**.[17]

The phosphine-thiolate hybrid ligands, $dmsp^-$ and $dpsp^-$, were found to stabilize the trithio(thiolato) structure of W(VI) in solution, because the additional phosphorus coordination prevents the molecules from degradation processes arising from coordinative unsaturation of trithio(thiolato) complexes, $(PPh_4)[(RS)W(S)_3]$. Another advantage of using such phosphine-thiolate hybrid ligands is that the electronic/steric properties of the complexes may readily be modified by the choice of phosphine substituents and by the length of hydrocarbons between sulfur and phosphorus atoms. The coordination site taken up by the phosphine group can be labile in solution as was noticed for **1b** (dpsp), and this hemilabile property may bestow new reactivity on the clusters derived therefrom. To this end, we anticipate that the trithiotungsten complexes having phosphine-thiolate hybrid ligands will provide us with a new tool to construct heterometallic sulfide clusters having structural diversity and new reactivity.

Supporting Information Available: Listings of X-ray crystallographic files in CIF format for the complex of **1a**,**b** and **2**−**5**. This material is available free of charge on the Internet at http://pubs.acs.org.

IC010921Q

(16) Huang, Q. W. X.-T.; Wang, Q.-M.; Sheng, T.-L.; Lu, J.-X. *Inorg. Chem.* **1996**, *35*, 893−897.

(17) (a) Kawaguchi, H.; Lang, J.-P.; Tatsumi, K. Unpublished result. (b) Kawaguchi, H. Ph.D. Thesis, Nagoya University, 1996.